Food and Chemical Toxicology 134 (2019) 110830

Contents lists available at ScienceDirect

Food and Chemical Toxicology

journal homepage: www.elsevier.com/locate/foodchemtox

α-Humulene inhibits hepatocellular carcinoma cell proliferation and induces apoptosis through the inhibition of Akt signaling

Hao Chen[a,b,1], Jingquan Yuan[b,c,**,1], Ji Hao[b], Yanzhang Wen[b], Yibing Lv[b], Lu Chen[c], Xinzhou Yang[a,*]

[a] School of Pharmaceutical Sciences, South-Central University for Nationalities, Wuhan, 430074, China
[b] Guangxi Scientific Research Center of Traditional Chinese Medicine, Guangxi University of Chinese Medicine, Nanning, 530001, China
[c] Guangxi Institute of Medicinal Plant, Nanning, 530023, China

ARTICLE INFO

Keywords:
α-Humulene
Hepatocellular carcinoma
Cytotoxicity
Apoptosis
Akt

ABSTRACT

Hepatocellular carcinoma (HCC) is a prevalent malignancy and a leading cause of cancer-related mortality. α-Humulene (HML) is a natural 11-membered monocyclic terpene with three E-configured double bonds isolated from *Eupatorium odoratum* L. We recently showed that HML has significant anti-HCC activity *in vitro* and *in vivo*. We found that HML was cytotoxic to HCC cells and induced mitochondrial apoptosis of HCC cells, promoting caspase-3 activation and PARP cleavage. HCC cells show abnormal Akt signaling to resist apoptosis. Mechanistically, HML was found to inhibit Akt activation, subsequently decreasing GSK-3 and Bad phosphorylation, promoting apoptotic induction. HML also inhibited cell proliferation and enhanced apoptosis in HCC tumor xenografts further highlighting its activity *in vivo*. Although HML showed minimal cytotoxicity to normal hepatocytes, weight loss was observed in mice administered HML. Taken together, these data provide important and novel insights into the anti-HCC effects of HML through its ability to inhibit Akt, reduced HCC cell proliferation, and enhanced HCC cell apoptotic induction *in vitro* and *in vivo*.

1. Introduction

Hepatocellular carcinoma (HCC) is the third leading cause of cancer related death globally (Siegel et al., 2015). Poor diagnostic tools and subsequent late stage diagnosis combined with the lack of efficient chemotherapeutic treatments contributes to poor survival in HCC patients (Finn et al., 2018; Mittal et al., 2016). More effiective HCC diagnostics and anti-HCC therapies are therefore urgently required.

Protein kinase B (Akt) is a serine/threonine-protein kinase that plays a major role in cell growth, survival, and frequently involves in carcinogenesis as a proto-oncogene (Mayer and Arteaga, 2016). Akt is activated through phosphorylation within its carboxy terminus at Ser473. The typical Akt phosphorylation targets include Bad, c-Raf, caspase-9, GSK-3α/β and TSC2, all of which are associated with cell proliferation and survival (Manning and Cantley, 2007). Akt has received intense research interest due to its frequent dysregulation in human cancers including HCC (Hennessy et al., 2005). The majority of HCC patients with a poor prognosis display hyperphosphorylated Akt in tumor cells, with no aberrant Akt activation observed in non-tumor tissue or normal hepatocytes (Chen et al., 2009; Su et al., 2016). Mutations in Akt and its upstream regulators can enhance Akt hyperactivity in tumors (Zucman-Rossi et al., 2015). Furthermore, it has shown that the dysregulation of Akt signaling promotes cancer cell survival and chemotherapy resistance (Altomare and Testa, 2005; Martini et al., 2014). These findings suggest that Akt is a prospective therapeutic target in HCC.

In this study, α-Humulene (HML), a natural 11-membered monocyclic terpene with three E-configured double bonds was purified from *Eupatorium odoratum* L. (EO) plants. Essential oils containing HML have been shown to possess antineoplastic properties (Loizzo et al., 2007; Sylvestre et al., 2005, 2006) but the effects of HML on HCC have not been studied in detail. We demonstrate that HML inhibits HCC cell

Abbreviations: HCC, hepatocellular carcinoma; *Eupatorium odoratum* L, EO; HML, α-Humulene; CDDP, cisplatin; FACS, fluorescence-activated cell sorting; Tunel, terminal deoxynucleotidyl transferase dUTP nick end labeling; IHC, immunohistochemistry; Caspase-3, cysteinyl aspartate-specific proteinases 3; PARP, poly ADP-ribose polymerase; Akt, serine/threonine-specific protein kinase

* Corresponding author.
** Corresponding author. Guangxi Scientific Research Center of Traditional Chinese Medicine, Guangxi University of Chinese Medicine, Nanning, 530001, China.
E-mail addresses: yjqgx@163.com (J. Yuan), xzyang@mail.scuec.edu.cn (X. Yang).
[1] These authors contributed equally to this work.

https://doi.org/10.1016/j.fct.2019.110830
Received 25 April 2019; Received in revised form 11 September 2019; Accepted 17 September 2019
Available online 25 September 2019
0278-6915/

proliferation and induces HCC cell apoptosis both *in vitro* and *in vivo*. We further show that HML inhibits Akt signaling, explaining its apoptotic and antiproliferative effects on HCC cells. Collectively, this study highlights the potential therpeutic benefits of HML to future anti-HCC treatment regimens.

2. Material and methods

2.1. Chemical elucidation of HML

The isolated compound from the plant species *Eupatorium odoratum* L. was identified as α-Humulene (HML) by comparison with NMR with the published reference data (Neuenschwander et al., 2012). Mass spectra and NMR of HML could be found in Supplementary Figs. 1–3.

2.2. Chemical reagents and antibodies

HML was dissolved (50 mg/mL) in DMSO as a stock solution, stored at −20 °C, and diluted with medium before each experiment. Wortmannin and insulin (human) were purchased from MedChem Express (Guangzhou, China). Cisplatin (CDDP) was purchased from Sigma-Aldrich (Shanghai, China). DMSO, PBS and Sodium dodecyl sulfate polyacrylamide gel kit were purchased from Solarbio (Beijing, China). The primary antibodies including anti-p53, anti-p21 Waf1/Cip 1, anti-Cyclin D1, anti-caspase-3, anti-PARP, anti-phosphorylation-Akt (Ser473), anti-Akt, anti-phosphorylation-GSK-3α/β (Ser 21/9), anti-GSK-3α/β, anti-phosphorylation-Bad (Ser136), anti-Bad and anti-β-actin were purchased from Cell Signaling Technology (MA, USA). The secondary antibodies of anti-mouse IgG and anti-rabbit IgG were purchased from ABclonal (Wuhan, China).

2.3. Cell culture

Huh7, SMMC-7721, HepG2 and Hep3B cells are HCC cells lines of human origin. L0-2 cells are normal hepatic cell line. HepG2 and Hep3B were purchased from the American Type Culture Collection (Manassas, VA, USA); Huh7, SMMC-7721 and L0-2 were purchased from the Library of Typical Culture of Chinese Academy of Sciences (Shanghai, China). After cell thawing, the cells were cultured in Dulbecco's modified Eagle's medium (DMEM; Sigma-Aldrich, Shanghai, China), supplemented with 10% fetal bovine serum and 1% penicillin/streptomycin (Hyclone, UT, USA). All cells were maintained in 25 cm^2 or 75 cm^2 cell culture flasks in a humidified atmosphere containing 5% CO_2 at 37 °C.

2.4. Crystal violet staining assay

Crystal violet staining assay was performed as described previously (Raj et al., 2011). Huh7, SMMC-7721, HepG2 and Hep3B cells were seeded into 12-well plates and allowed to grow to confluency of 60–70%, and then the cells were incubated with DMSO (1‰ V/V), HML or CDDP for 24 h while DMSO-treated group was served as control. Following the treatment time, mediums were removed; cells were then washed by PBS and fixed in 3.7% formaldehyde for 15 min before staining with crystal violet stain (Beyotime, Shanghai, China) for visual quantification of cell viability.

2.5. Cell cytotoxicity by CCK-8 assay

CCK-8 assay was performed following the kit protocol (Beyotime, Shanghai, China). Equal numbers of Huh7, SMMC-7721, HepG2, Hep3B and L02 cells were seeded into 96-well plates and allowed to grow for 24 h, and then the cells were incubated with DMSO (1‰ V/V), HML or CDDP for 6, 12 or 24 h while DMSO-treated group was served as control. Following the treatment time, mediums were removed, and cells were then incubated in fresh DMEM with CCK-8 for additional 3 h before measuring the optical density under 450 nm by spectrophotometer (Thermo Scientific, Vantaa, Finland). Cell inhibition rate was established utilizing the following Equation:

$$\text{Inhibition rate } (\%) = [1 - (OD_{sample} - OD_{blank})/(OD_{control} - OD_{blank})] \times 100$$

The IC_{50} value is defined as 50% inhibitory concentrations determined by CCK-8 assays and obtained by linear regression analysis using GraphPad Prism 6.0 Software.

2.6. Trypan-blue exclusion assay

Trypan-blue exclusion assay was performed as described previously (Raj et al., 2011). Equal numbers of Huh7, SMMC-7721, HepG2 and Hep3B cells were seeded into 6-well plates and allowed to grow to confluency of 70–80%. Then the cells were incubated with DMSO (1‰ V/V) or HML for 6, 12 or 24 h while DMSO-treated group was served as control. Following the treatment time, cells were then collected and stained with trypan blue (Beyotime, Shanghai, China). The viable and dead cells (stained by trypan blue) were counted by a hematocytometer. The percentage of viable cells was plotted graphically with histogram for quantification of cell viability.

2.7. Histological morphology and Hoechst 33258 staining

Histological morphology and Hoechst 33258 staining were performed as described previously (Chen et al., 2018). HepG2, Hep3B and L-02 cells were seeded into 6-well plates, and allowed to grow to confluency of 70–80%. Then the cells were incubated with DMSO (1‰ V/V) or HML for 12 h while DMSO-treated group was served as control. Following the treatment time, the cells were photographed at a magnification of 200 × /400 × under a phase contrast microscope (Leica, Nussloch, Germany), and the cells were then washed by PBS and fixed in methanol/acetic acid (3 : 1) for 15 min before stained with Hoechst 33258 (Beyotime, Shanghai, China). Subsequently, the cells were photographed at a magnification of 200 × /400 × under a fluorescence microscope (Leica, Nussloch, Germany).

2.8. Protein preparation and Western blot analysis

HepG2 and Hep3B were seeded into 100 mm × 20 mm cell culture dishes and allowed to grow to confluency of 60–70%. Then the cells were incubated with designated solutions for 6 or 12 h while DMSO-treated group was served as control. Following the treatment time, cells or xenografts were collected and lysed in RIPA containing phenylmethanesulfonyl fluoride and PhosSTOP (Solarbio, Beijing, China). The supernatant containing protein was collected and stored at −80 °C until use. The measurement of protein contents was performed with a BCA kit (Beyotime, Shanghai, China). Equivalent amounts of the proteins were separated by SDS-PAGE and transferred to polyvinylidine difluoride membranes (Bio-Rad, CA, USA). The membranes were blocked by 5% skim milk in tris-buffered saline with tween 20 (0.5%) for 2 h. Subsequently, the membranes were incubated with the primary antibody at 4 °C overnight and incubated with the secondary antibody at 37 °C for 2 h. The HRP ECL system (Beyotime, Shanghai, China) was used to visualize the protein band and the gray value was analyzed by Quantity One software.

2.9. FACS (Annexin-V FITC/PI staining)

HepG2 and Hep3B were seeded into 6-well plates and allowed to grow to confluency of 60–70%, then the cells were incubated with designated solutions for 6 or 12 h; DMSO-treated group served as control. Following the treatment time, cells were collected and stained. Annexin-V FITC/PI staining was performed following kit protocol

(Beyotime, Shanghai, China). Proportion of apoptotic cells were analyzed by cytometer (BD Biosciences, USA) and FlowJo V10 software.

2.10. HCC-bearing nude mice model and in vivo administration

HepG2-bearing nude mouse model was established as described previously (Su et al., 2011). Briefly, 200 μL of HepG2 cells (1×10^7 per mouse) were subcutaneously transplanted into the right flank of the nude mice (BALB/c, SPF grade, Female, 16–18 g, 4–5 weeks old). When tumors reached 100 mm^3, the animals were randomized in 4 groups (n = 5 mice per group) and treated intraperitoneal injection (i.p.) with HML (10, 20 mg/kg/2 days) for 4 weeks. Body weight was measured every 2 days; tumor size was measured every 4 days. Following the treatment time, mice were sacrificed; whole blood samples were collected for hematology; vital organs were dissected out and weighed; transplanted tumors were removed for assessments. All protocols involved in our animal experiments were in accordance with the protocols approved by the Animal Care and Use Committee of South-Central University for Nationalities (Wuhan, China).

2.11. Terminal deoxynucleotidyl transferase dUTP nick end labeling assay (TUNEL)

Xenografts were embedded in paraffin and cut into sections (5 μm) after pretreatment with ice-cold saline and fixed in buffered neutral 10% formalin. The sections were stained following TUNEL assay kit protocol (Roche Biotechnology, Basel, Switzerland) before photographing at the magnification of 200 × /400 × . Apoptosis index was quantified by the yellow-stained apoptotic nucleus. Ten regions were chosen from the photographs of tumor sections randomly, then blinded and counted by two people. Their mean values were used in statistical analysis. To avoid the discrepancy between two observers, a datum was valid only if the discrepancy between the two observers was less than 10%.

2.12. Immunohistochemical examinations of transplanted tumor tissues (IHC)

Immunohistochemical examinations were conducted as described previously (Fang et al., 2014). Briefly, after embedding in paraffin, xenografts were cut into sections (5 μm) and incubated with the designated primary antibodies, and visualized by corresponding secondary antibodies before photographing at the magnification of 200 × /400 × . Positive staining was quantified by Image J software.

2.13. Statistical analysis

All data are shown as mean ± SD from three independent experiments. GraphPad Prism 6.0 software was used for analysis. Statistically differences were analyzed using one-way analysis of variance (ANOVA) and *P*-values < 0.05 were considered significant.

3. Results

3.1. HML inhibits the proliferation of HCC cells in vitro

HML is a natural sesquiterpene isolated from Eupatorium odoratum L. (Supplementary Fig. 2A). Essential oils that possess antineoplastic properties contain HML as their active ingredient (Legault et al., 2003), but the effects of HML on HCC and its anti-tumor mechanisms are poorly understood. In this study, we examined the effects of HML on HCC cells and normal hepatocytes. HML treatment, like CDDP treatment (10 μg/mL), significantly induced cell death in the HCC cell lines (Huh7, SMMC-7721, HepG2 and Hep3B) at 15 μg/mL (Fig. 1A). CCK-8 assays showed that the IC_{50} values of HML were 15.09 ± 1.84, 17.31 ± 2.03, 11.22 ± 1.25 and 13.78 ± 1.46 μg/mL in Huh7, SMMC-7721, HepG2 and Hep3B respectively and 115.69 ± 3.52 μg/mL in normal hepatocytes (L-02) in 12 h. These data showed that the cytotoxicity of HML in normal hepatocytes significantly lower in HCC cells, suggesting cancer-selective cytotoxicity (Fig. 1B). Photomicrographs further showed that HML treatment induced HCC cell shrinkage, distortion, and a loss of the cellular matrix with no obvious effects on L-02 cells (Fig. 1C). Both inhibition curves and cell viability assays indicated that HML inhibited HCC cells in a concentration- and time-dependent manner (Fig. 1D and E). Notably, HepG2 expresses wild-type p53 and p21 but Hep3B is p53 defective. In this study, we found that cytotoxic effects of HML both occurred in HepG2 and Hep3B, while HepG2 was more sensitive to HML. Western blot analysis further showed that the expression of the antiproliferative proteins p53 and p21 was enhanced by HML, with an accompanying decrease in Cyclin D1 expression in HepG2 cells. As expected, p53 was undetectable in Hep3B cells, but the induction of Cyclin D1 expression was decreased accompanying a slight increase of p21, suggested HML-mediated antiproliferation in Hep3B cells was a p53-independent event. (Supplementary Fig. 4). These results indicated that HML preferentially inhibits the proliferation of HCC cells and the sensitivity of HML-induced antiproliferation was modulated by the expression of p53.

3.2. HML inhibits HepG2 cell proliferation in xenograft nude mouse models

The *in vivo* anti-HCC effects of HML were evaluated in a HepG2-bearing nude mouse model. When the tumor volume grew to 100 mm^3, HML was administered i. p. every 2 days for 4 weeks. Significant growth inhibition of the HepG2 xenografts was observed in HML-administered HepG2-bearing mice (Supplementary Fig. 5, Fig. 2A and B). HML treatment decreased the tumor weights in a dose-dependent manner compared to DMSO-controls, and in a degree comparable to CDDP (Fig. 2C). To detect potential toxic side-effects, we monitored body weight every two days and collected whole blood samples as well as vital organs for hematology and organ index analysis. Although HML and CDDP treatment were not lethal, both compounds increased weight loss in the mice, compared to DMSO-treated controls. The weight loss was more pronounced in CDDP compared to HML treated mice (Supplementary Fig. 6). No obvious differences in blood biochemical parameters or organ indices were evident between DMSO- and HML-treated groups. CDDP led to greater liver and kidney damage in comparison to HML (Supplementary Tables 1 and 2). Taken together, these data suggest that HML has fewer toxic effects on HepG2-bearing nude mice than CDDP, but some weight loss does occur following HML treatment.

3.3. HML induces HCC cell apoptosis in vitro

The data thus far suggested that HML can induce apoptosis in HCC cells. To investigate the potential apoptotic effects of HML, HepG2 and Hep3B cells were treated with 10 and 15 μg/mL HML (base on the IC_{50} values determined by CCK-8 assay) for 12 h. We found that the apoptotic characteristics triggered by CDDP (chromatin condensation and apoptotic body) were also observed in HML-treated HCC cells (Fig. 3A). FACS analysis of PI and Annexin-V stained cells confirmed that HML treatment resulted in an increased apoptotic populations (Q2 and Q3) to a greater degree than CDDP (Fig. 3B). Cleavage of caspase-3 and PARP is essential for apoptosis as an activated form (Yap et al., 2011). Western blot analysis showed that HML induced the cleavage of caspase-3 and PARP (Fig. 3C) in a concentration dependent manner confirming its apoptotic effects on HCC cells *in vitro*. These results suggested that HML showed pro-apoptotic effects on HCC cells.

3.4. HML induced HepG2 xenograft apoptosis in nude mouse models

Given the pro-apoptotic activity of HML against HCC cells *in vitro*, we next examined its *in vivo* effects. Xenografts were collected from

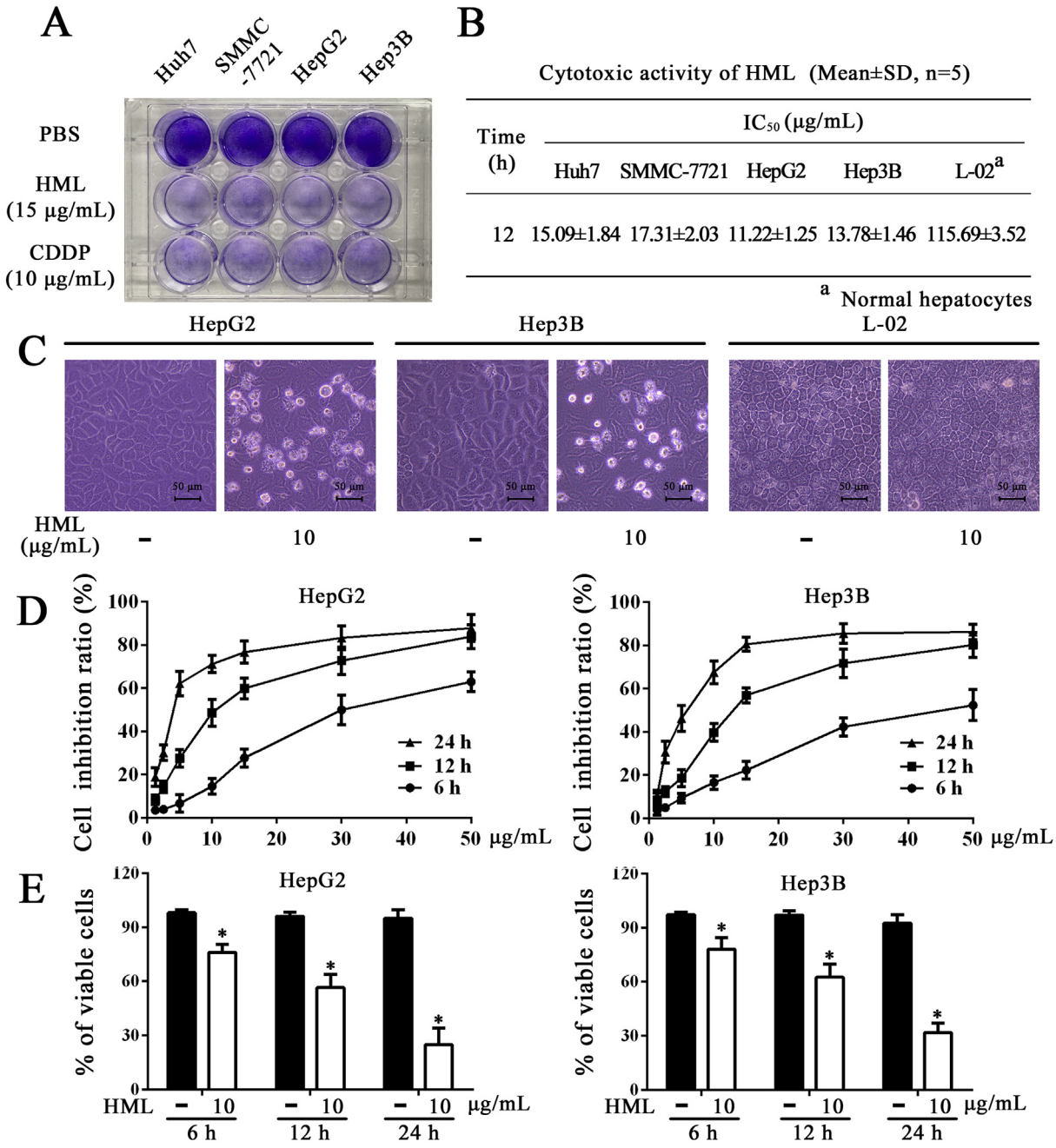

Fig. 1. HML inhibits the proliferation of HCC cells *in vitro*. (A) Crystal violet cell viability staining of HCC cells (Huh7, SMMC-7721, HepG2 and Hep3B) following HML (15 μg/mL) or CDDP (10 μg/mL) treatment for 24 h. (B) The cancer-selective cytotoxic effects of HML. HCC cells and normal hepatocytes (L-02) were grown in 96 well plates and treated with HML at 1.25–150 μg/mL for 12 h. Cytotoxicity assessed through CCK-8 assays, and IC_{50} values were calculated. The cytotoxic effects of HML in normal hepatocytes were significantly lower in HCC cells. (C) Morphological observations of HepG2, Hep3B and L-02 cells following HML treatment. HML induced HepG2 and Hep3B cells shrinkage, distortion and a loss of the cellular matrix with no obvious impact on L-02 cells at the effective concentrations. (D) HML exhibited significant cytotoxicity in HepG2 and Hep3B cells in a concentration- and time-dependent manner. HepG2 and Hep3B cells were grown in 96 well plates and treated with HML at 1.25–50 μg/mL for 6, 12 or 24 h. Cytotoxicity assessed through CCK-8 assays, and IC_{50} values were calculated. (E) HML inhibits HCC cell viability in a time dependent manner. Viability was measured by trypan-blue exclusion assays. Statistical analysis was performed using a one–way ANOVA, $^{*}P < 0.05$. (For interpretation of the references to colour in this figure legend, the reader is referred to the Web version of this article.)

HepG2-bearing nude mice and visualized by HE, TUNEL staining, and IHC. HE staining showed that HML treatment caused tumor chromatin condensation and a loss of tumor structure. TUNEL staining revealed that HML led to a dose-dependent increase in apoptotic cells in the xenograft sections. Similar results were observed for IHC staining. HML- and CDDP-treated xenograft samples exhibited high levels of caspase-3 cleavage compared to DMSO-treated tumor samples (Fig. 4A). Western blot analysis and IHC staining suggested that HML-induced apoptosis through the intrinsic mitochondrial caspase cascade (Fig. 4B). Taken together, these results indicated that HML can induce HCC cell apoptosis *in vitro* and in HepG2-bearing nude mouse models through mitochondrial associated apoptotic pathways.

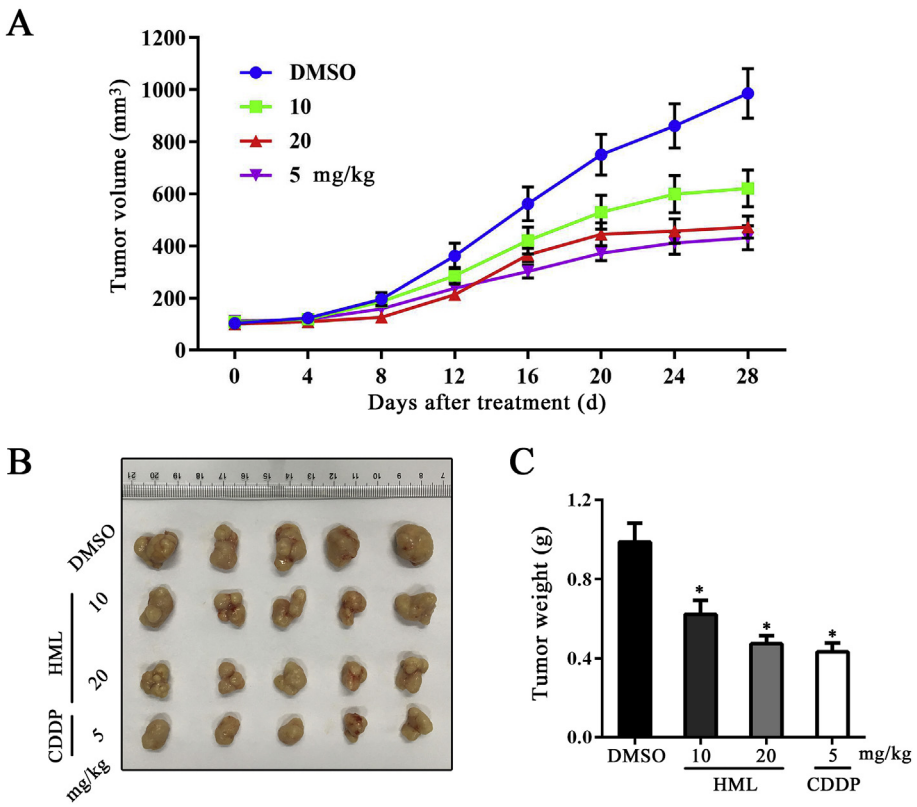

Fig. 2. HML inhibits HepG2 cell growth in xenograft nude mouse models. When the tumor volume reached 100 mm^3, HML (10 mg/kg or 20 mg/kg) or DMSO (5% V/V) were administered i. p. every 2 d for 4 weeks; CDDP (5 mg/kg) was administered as a positive control i. p three times a week, for 4 weeks. (A and B) Tumor volumes were measured every 4 d after implantation. HML administration reduced tumor growth. (C) Nude mice were sacrificed and xenografts were dissected for weight measurements. Statistical analysis was performed using a one way-ANOVA, $*P < 0.05$.

3.5. HML inhibits Akt signaling

3.5.1. HML reduces Akt activity in HCC cells

The PI3K-Akt signaling axis suppresses cell apoptosis and Akt is frequently hyperphosphorylated in cancer cells. Our data shows that HML inhibited p53-wild-type/defective HCC cells. Interestingly, we observed the increase in p21 and the accompanying decrease in Cyclin D1 in both HepG2 and Hep3B. Previously, several molecular targets of Akt, including p21 and Cyclin D1 associated with the proliferation have been assessed (Kakuda et al., 2009; Li et al., 2018). We therefore investigated the effects of HML on Akt signaling. Western blot analysis showed that HML treatment downregulated the phosphorylation of Akt in a concentration dependent manner, which was accompanied by decreased GSK-3α/β and Bad phosphorylation, most notably in HepG2 cells. Wortmannin was included as a known PI3K inhibitor (Dienstmann et al., 2014) in these assays and showed comparable levels of p-Akt inhibition in HepG2 cells (Supplementary Fig. 7A, Fig. 5A). We further measured the levels of p-Akt in xenograft tissue. Similarly, HML administration inhibited p-Akt, p-Bad and p-GSK-3α/β levels in the tumor tissues of nude mouse models (Supplementary Fig. 7B, Fig. 5B) confirming that the effects of HML are conserved *in vivo* (Fig. 5C). These results confirmed that HML inhibits Akt activation, which may contribute to its anti-HCC effects.

3.5.2. Akt inhibition of HML induces HCC cell apoptosis and inhibits cell proliferation

To investigate if the inhibition of Akt mediates HML-induced HCC cell apoptosis, we used insulin to stimulate p-Akt (Zhang et al., 2017) in HepG2 and Hep3B cells co-treated with a range of HML concentrations. Akt related proteins were quantified by Western blot analysis, HCC cell apoptosis was measured by FACS, and HCC cell viability was assessed via trypan-blue exclusion assays. Western blot analysis showed that the inhibition of p-Akt by HML was partially reverse by insulin treatment, which led to increased p-Akt, p-Bad, and p-GSK-3α/β levels (Supplementary Fig. 8, Fig. 6A). Moreover, the effects of HML on HCC cell apoptosis and proliferation were partially reversed by insulin treatment (Fig. 6B and C). Collectively, these results demonstrate that Akt inhibition mediates the effects of HML on HCC cell apoptosis and proliferation.

4. Discussion

Plant essential oils are an important source of anticancer natural products, the activity of which generally originates from terpenoids (Gautam et al., 2014; Rabi and Bishayee, 2009). In this study, HML, a natural 11-membered monocyclic terpene with three E-configured double bonds, was isolated from the plant species *Eupatorium odoratum* L. HML is widely distributed in the essential oils of various plants. Interestingly, these essential oils containing HML have known antineoplastic properties while the anti-cancer effects of HML appear to be tumor-selective (Costa et al., 2015; Da Silva et al., 2007; El Hadri et al., 2010; Legault et al., 2003; Loizzo et al., 2008). Recently, some antioxidant agents including Vitamin C, Vitamin E, Trolox and NAC (Piskounova et al., 2015; Sayin et al., 2014; Schafer et al., 2009; Subramani et al., 2014; Velauthapillai et al., 2017) and regulators of antioxidant pathway (Wang et al., 2016) were found to promote metastasis or survival by decreasing the inhibition from ROS in cancer. HML thus may pose a survival strategy for cancer cells. To definitively investigate whether HML has anti-HCC activity, we investigated its cytotoxicy and anti-proliferative effects in an array of HCC cell lines *in vitro*. Our data revealed that HML has selective killing properties among HCC cell lines and hepatocytes, and exhibited concentration- and time-dependent antiproliferative effects on HepG2 and Hep3B cells. Similar result can observe in a preliminary literature, which suggested that HML treatment induced a decrease in cellular GSH content and an increase in ROS production, which may be implicated in its cytotoxicity (Legault et al., 2003). Furthermore, HepG2-bearing nude mouse models were used to confirm the *in vivo* anti-HCC effects of HML. Significant antiproliferative effects on xenograft models were observed in HML-administered HepG2-bearing mice, indicating that HML has favorable

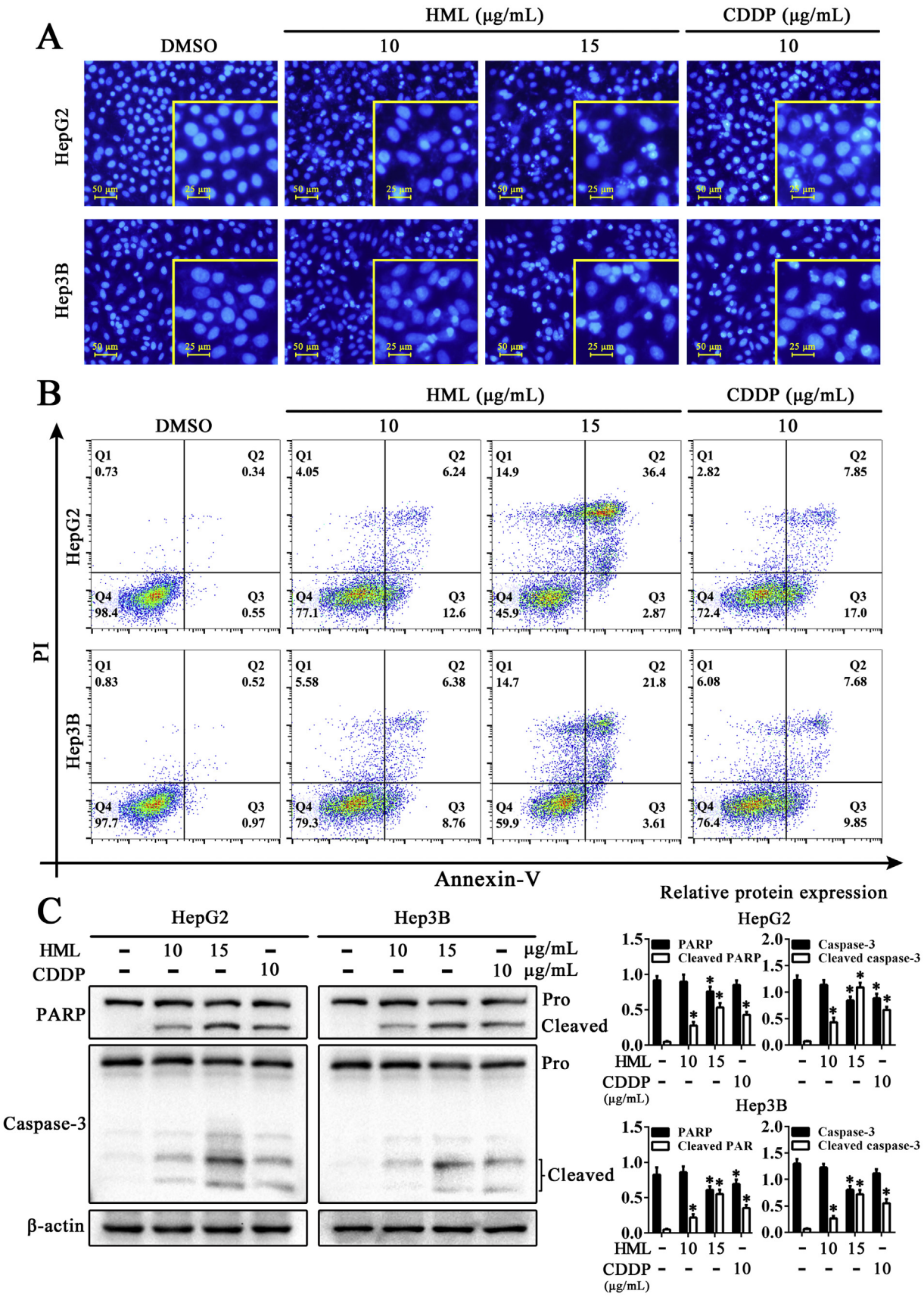

Fig. 3. HML induces HCC cell apoptosis *in vitro*. (A) Hoechst 33258 staining of HepG2 and Hep3B cells. Hoechst 33258 was used to stain nuclear DNA. Following HML or CDDP treatment for 12 h, the HCC cell nuclei showed apoptotic characteristics (chromatin condensation and the formation of apoptotic bodies). (B) FACS (PI and Annexin-V) analysis of HML-treated HCC cells. HML treatment resulted in increased numbers of apoptotic populations in a concentration-dependent manner. (C) Effects of HML on mitochondrial apoptotic proteins were analyzed by Western blot analysis in HepG2 and Hep3B cells. HML treatment led to caspase-3 activation and PARP cleavage in HCC cells. Statistical analysis was performed using a one-way ANOVA, $^{*}P < 0.05$.

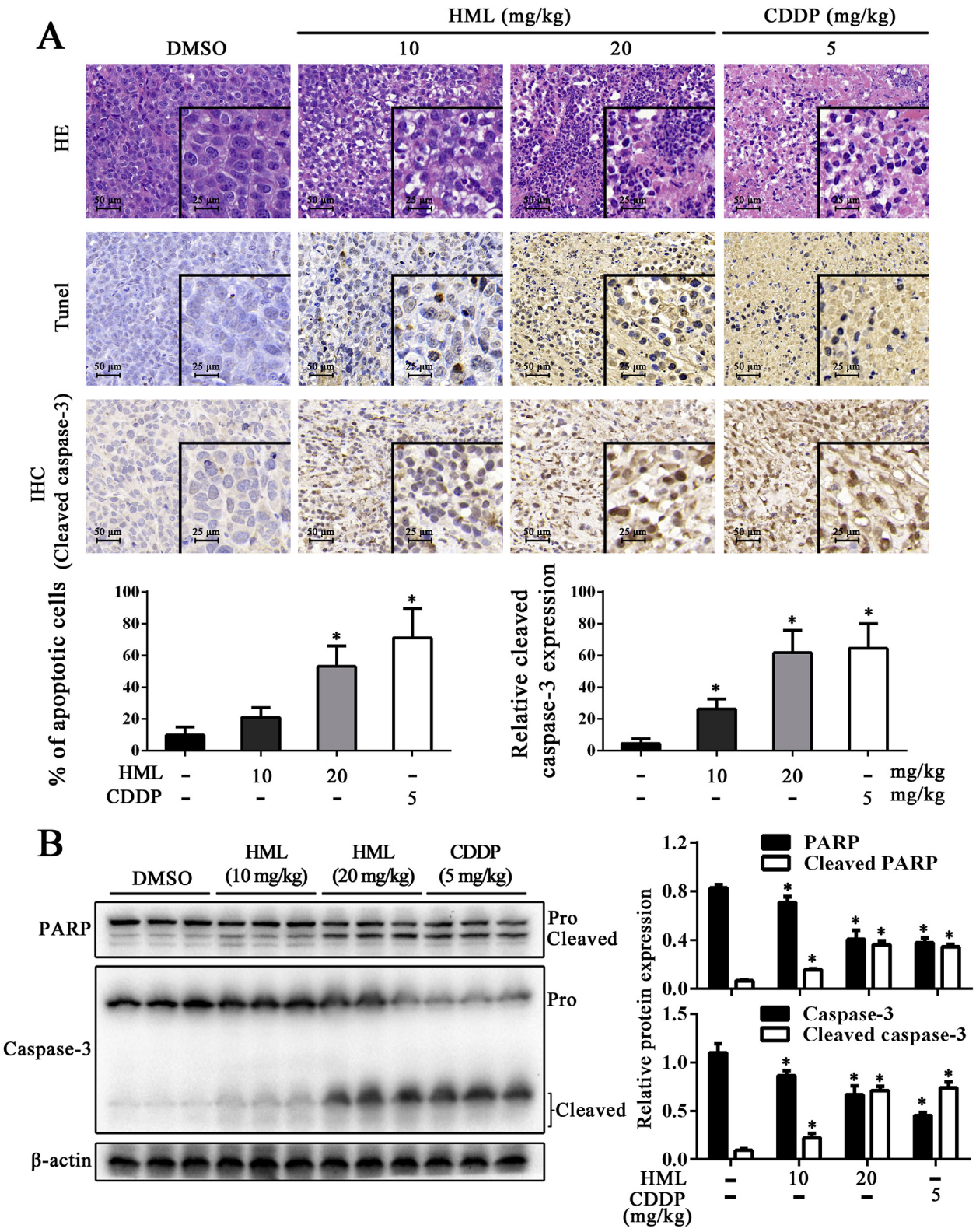

Fig. 4. Pro-apoptotic effects of HML in HepG2-bearing nude mouse models. (A) Tumor sections of HepG2-bearing nude mouse models were prepared and subjected to HE staining, TUNEL staining, and IHC. HE-stained tumor tissue sections were used for histological analysis. Quantification of apoptotic cells was determined by TUNEL staining. Cleaved caspase-3 levels were visualized and quantified by IHC. HML-treated sections showed chromatin condensation and a loss of structural integrity. Similar observations were observed in CDDP-treated sections. HML treatment increased the proportion of apoptotic cells in HCC tissues. High levels of cleaved caspase-3 staining were also observed in HML-treated samples. (B) Effects of HML on mitochondrial apoptotic proteins were analyzed by Western blot in xenograft lysates. Similarly, HML administration promoted the cleavage of caspase-3 and PARP *in vivo*. Statistical analysis was performed using a one-way ANOVA, $^{*}P < 0.05$.

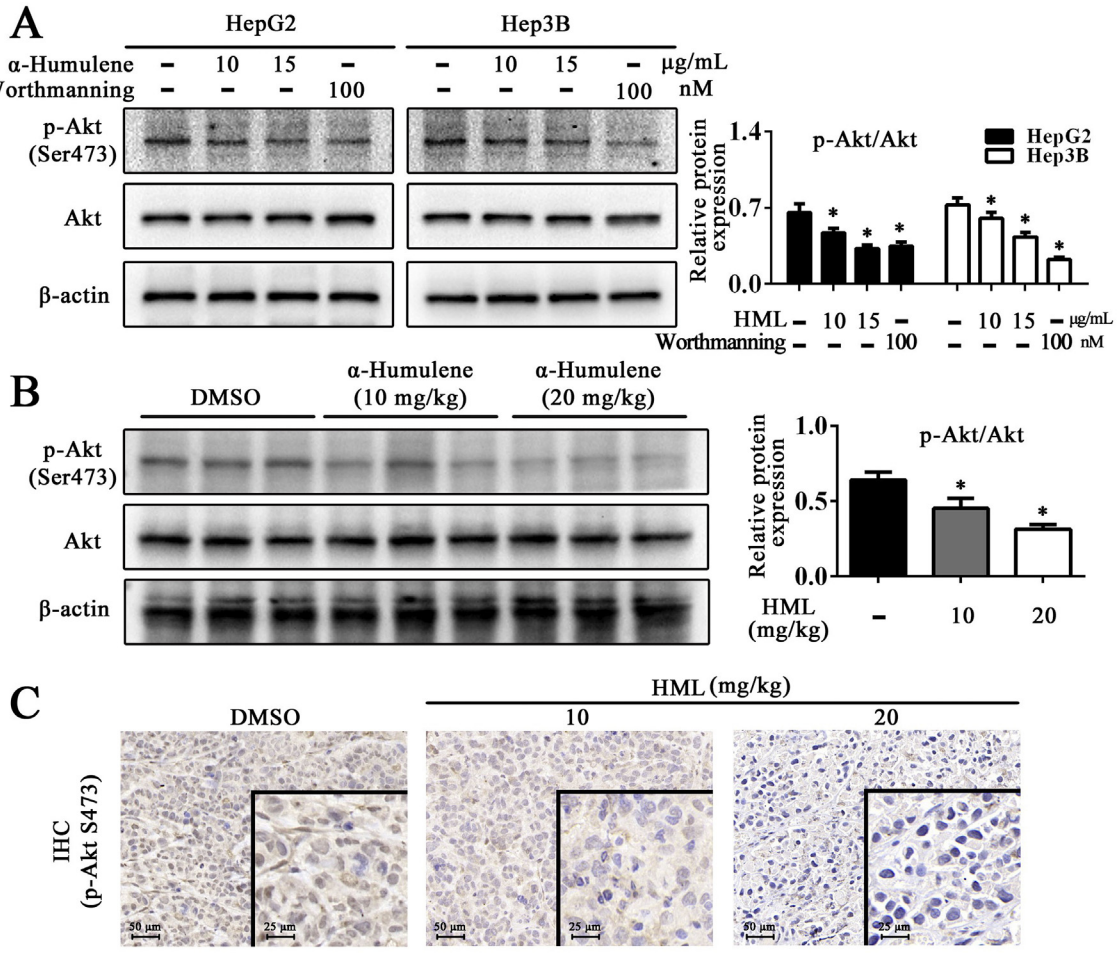

Fig. 5. HML inhibits Akt activity in HCC cells and tumor tissues. (A) Effects of HML on Akt and its targets Bad and GSK-3α/β were analyzed by Western blot in HepG2 and Hep3B cells. HML treatment inhibited the phosphorylation of Akt at Ser473, which was accompanied by a decrease in the phosphorylation of Bad and GSK-3α/β. (B) Similar results were obtained in the tumor tissues of nude mouse models. (C) IHC observations show weak p-Akt (Ser473) staining in HML-treated tumor tissue sections. Statistical analysis was performed using a one-way ANOVA, $^{*}P < 0.05$.

anti-HCC activity *in vivo*. Conclusively, HML in our experimental concentration has not pose a survival strategy for HCC cells. In contrast, HML shows a chemotherapeutics potential to anti-HCC treatment.

We next focused on the systemic toxicological effects of HML in HepG2-bearing mice. CDDP is a conventional chemotherapeutic drug recommended for clinical HCC treatment, but its use is limited by several toxic side effects (Oun et al., 2018). Hematologic and viscera results showed that CDDP treatment induced significant nephrotoxicity and hepatotoxicity in nude mice. In contrast, no significant hematologic alterations in mice administered HML were observed when compared to DMSO-treated groups and non-tumor groups. It is worth noting that both of HML and CDDP treatment induced weight loss, though these effects were lower for HML compared to CDDP, suggesting HML had potential side effects. Previous studies suggested that the side effects of HML are associated with its metabolism, tissue distribution (Chaves et al., 2008) and ability to inhibit CYP3A (Nguyen et al., 2017).

The malignant transformation of HCC is driven by mutations in both oncogenes and tumor suppressor genes (Luo et al., 2009). Transformational cells with a large number of gene defects frequently manifest as enhanced cellular stress and an apoptotic fate. During the adaptation to cell stress, tumor cells enhance survival signals. Targeting these signals may enhance cytotoxic signaling, sensitizing tumor cells to apoptotic induction (Yap et al., 2011). Our preliminary study showed that HML has more potent antiproliferative and pro-apoptotic effects on HepG2 cells, but p53 defect did not completely blind its effects, suggested that more signaling mechanism remains related. Interestingly, we observed the increase in p21 and the accompanying decrease in Cyclin D1 in both HepG2 and Hep3B. Previous reports indicated that Akt acts as an upstream of p21 to encourage antiproliferation and cell death (Li et al., 2018; Tak et al., 2019). Akt also positively influences proliferation by preventing the GSK-3β mediated phosphorylation and degradation of Cyclin D1 (Manning and Cantley, 2007). Moreover, Akt can inhibit p53 through its ability to activate MDM2 (Matsuda et al., 2018). Basing on these findings, we inferred that the inhibition of Akt signaling may mediate the effects of HML on HCC cells. We further revealed that the phosphorylation of Akt in HCC cells was down-regulated by HML treatment. Apoptosis and proliferation are tightly regulated through a plethora of highly orchestrated signaling pathways. Akt is one such regulator that promoted cell survival and proliferation when phosphorylated at Ser473. Accordingly, tumor cells frequently display Akt hyperphosphorylation to resist cell stress and apoptosis. Active Akt inhibits apoptosis through the phosphorylation and inactivation of several pro-apoptotic proteins including Bad and caspase-9. Phosphorylation of Bad at Ser136 promotes its binding to 14-3-3 proteins and prevents the association between Bad and Bcl-2/Bcl-xL (Zha et al., 1996). To explore this theory, HCC cells were co-treated with insuling (an Akt activator) and treated with HML. HML showed weak antiproliferative and pro-apoptotic effects in insulin-treated HCC cells, indicating that HML induced HCC cell apoptosis and antiproliferative effects were mediated by Akt signaling (outlined in Fig. 7).

Akt is a frequently activated oncoprotein in human cancers and a common target for anticancer therapy. Akt is hyperactivated in tumor

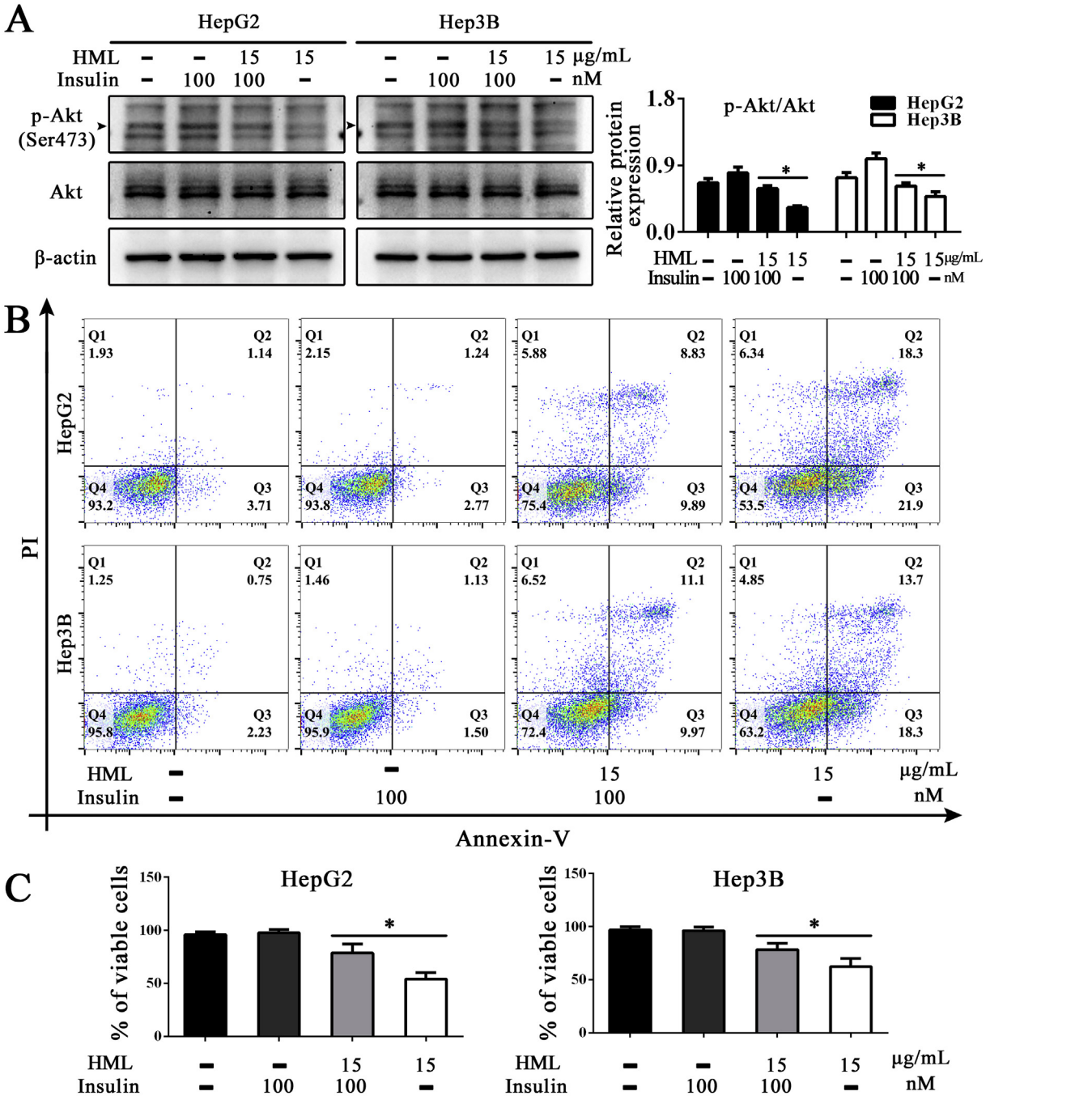

Fig. 6. AKT inhibition mediates HML-induced HCC cell apoptosis and its antiproliferative effects. (A) The inhibition of HML on Akt was partially reversed by insulin stimulation. HepG2 and Hep3B were incubated with DMSO (1‰ V/V), 100 nM insulin or 15 μg/mL HML alone or in combination for 6 h. Cell lysates were processed for Western blot analysis. (B) HCC cell apoptosis was measured by FACS (PI and Annexin-V). (C) Cell viability was measured by trypan-blue exclusion assay. Statistical analysis was performed using a one-way ANOVA, $^*P < 0.05$. (For interpretation of the references to colour in this figure legend, the reader is referred to the Web version of this article.)

cells by multiple mechanisms, inculding activating mutations in the catalytic subunits of PI3K, inactivating mutations in the tumor suppressor PTEN, and directly activating mutations in the Akt protein (Zucman-Rossi et al., 2015). Epidemiological studies show that steatohepatitis and virus infection are two high risk factors for hepatocarcinogenesis, both of which can activate Akt signaling in hepatocytes (Golob-Schwarzl et al., 2017; Liu et al., 2014). To-date, multiple clinical trials have supported this therapeutic strategy with HCC patients showing benefits when treated with Akt inhibitors (Dienstmann et al., 2014; Fruman and Rommel, 2014). These findings highlight the critical role of Akt in hepatocarcinogenesis and the progression of HCC, and strengthens the evidence that Akt signaling is a promising therpaeutic target for precision HCC treatment.

5. Conclusions

In summary, this study reports that HML has selective inhibitory effects on HCC by suppressing proliferation and inducing apoptosis *in vitro* and *in vivo*. Mechanistically, HML negatively regulates Akt signaling to inhibit HCC cell proliferation and promote apoptosis. HML therefore represents a novel and promising chemotherapy drug for precision HCC therapy.

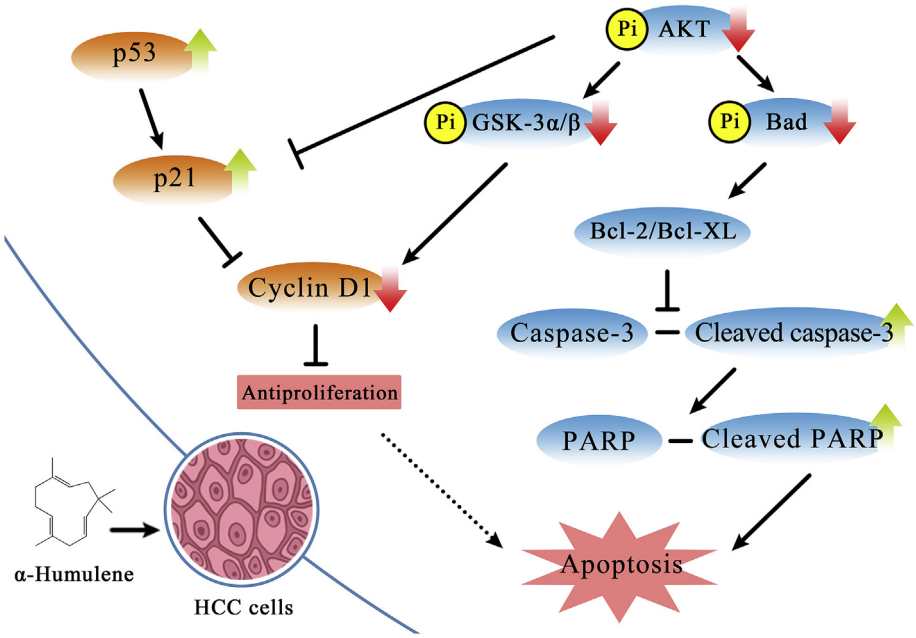

Fig. 7. The mechanism of HML-induced HCC apoptosis and antiproliferation.

Declaration of competing interest

The authors declare that they have no known competing financial interests or personal relationships that could have appeared to influence the work reported in this paper.

Acknowledgements

The work was financially supported by National Natural Science Foundation of China grants (81774000, 81660656 and 81573561) and Wuhan Applied Basic Research Program of Science and Technology (2017060201010217).

Appendix A. Supplementary data

Supplementary data to this article can be found online at https://doi.org/10.1016/j.fct.2019.110830.

References

Altomare, D.A., Testa, J.R., 2005. Perturbations of the AKT signaling pathway in human cancer. Oncogene 24, 7455. https://doi.org/10.1038/sj.onc.1209085.

Chaves, J.S., Leal, P.C., Pianowisky, L., Calixto, J.B., 2008. Pharmacokinetics and tissue distribution of the sesquiterpene α-humulene in mice. Planta Med. 74, 1678–1683. https://doi.org/10.1055/s-0028-1088307.

Chen, H., Zhou, B., Yang, J., Ma, X., Deng, S., Huang, Y., Wen, Y., Yuan, J., Yang, X., 2018. Essential oil derived from *Eupatorium adenophorum* Spreng. mediates anticancer effect by inhibiting STAT3 and AKT activation to induce apoptosis in hepatocellular carcinoma. Front. Pharmacol. 9. https://doi.org/10.3389/fphar.2018.00483.

Chen, J.s., Wang, Q., Fu, X.h., Huang, X.H., Chen, X.l., Cao, L.q., Chen, L.z., Tan, H.x., Li, W., Bi, J., 2009. Involvement of PI3K/PTEN/AKT/mTOR pathway in invasion and metastasis in hepatocellular carcinoma: association with MMP-9. Hepatol. Res. 39, 177–186. https://doi.org/10.1111/j.1872-034X.2008.00449.x.

Costa, E.V., Menezes, L.R., Rocha, S.L., Baliza, I.R., Dias, R.B., Rocha, C.A.G., Soares, M.B., Bezerra, D.P., 2015. Antitumor properties of the leaf essential oil of *Zornia brasiliensis*. Planta Med. 81, 563–567. https://doi.org/10.1055/s-0035-1545842.

Da Silva, S.L., Figueiredo, P.M., Yano, T., 2007. Chemotherapeutic potential of the volatile oils from *Zanthoxylum rhoifolium* Lam leaves. Eur. J. Pharmacol. 576, 180–188. https://doi.org/10.1016/j.ejphar.2007.07.065.

Dienstmann, R., Rodon, J., Serra, V., Tabernero, J., 2014. Picking the point of inhibition: a comparative review of PI3K/AKT/mTOR pathway inhibitors. Mol. Cancer Ther. 13, 1021–1031. https://doi.org/10.1158/1535-7163.

El Hadri, A., del Rio, M.G., Sanz, J., Coloma, A.G., Idaomar, M., Ozonas, B.R., González, J.B., Reus, M.I.S., 2010. Cytotoxic activity of α-humulene and transcaryophyllene from *Salvia officinalis* in animal and human tumor cells. An R Acad Nac Farm 76, 343–356.

Fang, Z., Tang, Y., Jiao, W., Xing, Z., Guo, Z., Wang, W., Xu, Z., Liu, Z., 2014. Nitidine chloride induces apoptosis and inhibits tumor cell proliferation via suppressing ERK signaling pathway in renal cancer. Food Chem. Toxicol. 66, 210–216. https://doi.org/10.1016/j.fct.2014.01.049.

Finn, R.S., Zhu, A.X., Farah, W., Almasri, J., Zaiem, F., Prokop, L.J., Murad, M.H., Mohammed, K., 2018. Therapies for advanced stage hepatocellular carcinoma with macrovascular invasion or metastatic disease: a systematic review and meta-analysis. Hepatology 67, 422–435. https://doi.org/10.1002/hep.29486.

Fruman, D.A., Rommel, C., 2014. PI3K and cancer: lessons, challenges and opportunities. Nat. Rev. Drug Discov. 13, 140. https://doi.org/10.1038/nrd4204.

Gautam, N., Mantha, A.K., Mittal, S., 2014. Essential oils and their constituents as anticancer agents: a mechanistic view. BioMed Res. Int. 2014. https://doi.org/10.1155/2014/154106.

Golob-Schwarzl, N., Krassnig, S., Toeglhofer, A.M., Park, Y.N., Gogg-Kamerer, M., Vierlinger, K., Schröder, F., Rhee, H., Schicho, R., Fickert, P., 2017. New liver cancer biomarkers: PI3K/AKT/mTOR pathway members and eukaryotic translation initiation factors. Eur. J. Cancer 83, 56–70. https://doi.org/10.1016/j.ejca.2017.06.003.

Hennessy, B.T., Smith, D.L., Ram, P.T., Lu, Y., Mills, G.B., 2005. Exploiting the PI3K/AKT pathway for cancer drug discovery. Nat. Rev. Drug Discov. 4, 988. https://doi.org/10.1038/nrd1902.

Kakuda, S., Shimura, T., Kuwahara, Y., Ochiai, Y., Takai, Y., Fukumoto, M., 2009. The AKT/cyclinD1 pathway is a novel target for overcoming radioresistance of tumor cells. In: The Japan Radiation Research Society Annual Meeting Abstracts the 52nd Annual Meeting of the Japan Radiation Research Society. The Japanese Radiation Research Society 96-96.

Legault, J., Dahl, W., Debiton, E., Pichette, A., Madelmont, J.-C., 2003. Antitumor activity of balsam fir oil: production of reactive oxygen species induced by α-humulene as possible mechanism of action. Planta Med. 69, 402–407. https://doi.org/10.1055/s-2003-39695.

Li, F., Jin, D., Tang, C., Gao, D., 2018. CEP55 promotes cell proliferation and inhibits apoptosis via the PI3K/Akt/p21 signaling pathway in human glioma U251 cells. Oncology letters 15, 4789–4796. https://doi.org/10.3892/ol.2018.7934.

Liu, L., Dong, Z., Liang, J., Cao, C., Sun, J., Ding, Y., Wu, D., 2014. As an independent prognostic factor, FAT10 promotes hepatitis B virus-related hepatocellular carcinoma progression via Akt/GSK3β pathway. Oncogene 33, 909. https://doi.org/10.1038/onc.2013.236.

Loizzo, M., Tundis, R., Menichini, F., Saab, A., Statti, G., Menichini, F., 2008. Antiproliferative effects of essential oils and their major constituents in human renal adenocarcinoma and amelanotic melanoma cells. Cell Prolif 41, 1002–1012. https://doi.org/10.1111/j.1365-2184.2008.00561.x.

Loizzo, M.R., Tundis, R., Menichini, F., Saab, A.M., Statti, G.A., Menichini, F., 2007. Cytotoxic activity of essential oils from *Labiatae* and *Lauraceae* families against in vitro human tumor models. Anticancer Res. 27, 3293–3299.

Luo, J., Solimini, N.L., Elledge, S.J., 2009. Principles of cancer therapy: oncogene and non-oncogene addiction. Cell 136, 823–837. https://doi.org/10.1016/j.cell.2009.02.024.

Manning, B.D., Cantley, L.C., 2007. AKT/PKB signaling: navigating downstream. Cell 129, 1261–1274. https://doi.org/10.1016/j.cell.2007.06.009.

Martini, M., De Santis, M.C., Braccini, L., Gulluni, F., Hirsch, E., 2014. PI3K/AKT signaling pathway and cancer: an updated review. Ann. Med. 46, 372–383. https://doi.org/10.3109/07853890.2014.912836.

Matsuda, S., Nakagawa, Y., Kitagishi, Y., Nakanishi, A., Murai, T., 2018. Reactive oxygen species, superoxide dimutases, and PTEN-p53-AKT-MDM2 signaling loop network in mesenchymal stem/stromal cells regulation. Cells-Basel 7, 36. https://doi.org/10.1016/j.cell.2009.02.024.

Mayer, I.A., Arteaga, C.L., 2016. The PI3K/AKT pathway as a target for cancer treatment. Annu. Rev. Med. 67, 11–28. https://doi.org/10.1146/annurev-med-062913-051343.

Mittal, S., Kanwal, F., Ying, J., Chung, R., Sada, Y.H., Temple, S., Davila, J.A., El-Serag, H.B., 2016. Effectiveness of surveillance for hepatocellular carcinoma in clinical practice: a United States cohort. J. Hepatol. 65, 1148–1154. https://doi.org/10.1016/j.jhep.2016.07.025.

Neuenschwander, U., Czarniecki, B., Hermans, I., 2012. Origin of regioselectivity in α-humulene functionalization. J. Org. Chem. 77, 2865–2869. https://doi.org/10.1021/jo3000942.

Nguyen, L.T., Myslivečková, Z., Szotáková, B., Špičáková, A., Lněničková, K., Ambrož, M., Kubíček, V., Krasulová, K., Anzenbacher, P., Skálová, L., 2017. The inhibitory effects of β-caryophyllene, β-caryophyllene oxide and α-humulene on the activities of the main drug-metabolizing enzymes in rat and human liver in vitro. Chem. Biol. Interact. 278, 123–128. https://doi.org/10.1016/j.cbi.2017.10.021.

Oun, R., Moussa, Y.E., Wheate, N.J., 2018. The side effects of platinum-based chemotherapy drugs: a review for chemists. Dalton Trans. 47, 6645–6653. https://doi.org/10.1039/C8DT00838H.

Piskounova, E., Agathocleous, M., Murphy, M.M., Hu, Z., Huddlestun, S.E., Zhao, Z., Leitch, A.M., Johnson, T.M., DeBerardinis, R.J., Morrison, S.J., 2015. Oxidative stress inhibits distant metastasis by human melanoma cells. Nature 527, 186. https://doi.org/10.1038/nature15726.

Rabi, T., Bishayee, A., 2009. Terpenoids and breast cancer chemoprevention. Breast Canc. Res. Treat. 115, 223–239. https://doi.org/10.1007/s10549-008-0118-y.

Raj, L., Ide, T., Gurkar, A.U., Foley, M., Schenone, M., Li, X., Tolliday, N.J., Golub, T.R., Carr, S.A., Shamji, A.F., 2011. Selective killing of cancer cells by a small molecule targeting the stress response to ROS. Nature 475, 231. https://doi.org/10.1038/nature10167.

Sayin, V.I., Ibrahim, M.X., Larsson, E., Nilsson, J.A., Lindahl, P., Bergo, M.O., 2014. Antioxidants accelerate lung cancer progression in mice. Sci. Transl. Med. 6 221ra215-221ra215. https://doi.org/10.1126/scitranslmed.3007653.

Schafer, Z.T., Grassian, A.R., Song, L., Jiang, Z., Gerhart-Hines, Z., Irie, H.Y., Gao, S., Puigserver, P., Brugge, J.S., 2009. Antioxidant and oncogene rescue of metabolic defects caused by loss of matrix attachment. Nature 461, 109. https://doi.org/10.1038/nature08268.

Siegel, R.L., Miller, K.D., Jemal, A., 2015. Cancer statistics, 2015. Ca - Cancer J. Clin. 65, 5–29. https://doi.org/10.3322/caac.21254.

Su, C.-L., Chen, F.-N., Won, S.-J., 2011. Involvement of apoptosis and autophagy in reducing mouse hepatoma ML-1 cell growth in inbred BALB/c mice by bacterial fermented soybean products. Food Chem. Toxicol. 49, 17–24. https://doi.org/10.1016/j.fct.2010.08.017.

Su, R., Nan, H., Guo, H., Ruan, Z., Jiang, L., Song, Y., Nan, K., 2016. Associations of components of PTEN/AKT/mTOR pathway with cancer stem cell markers and prognostic value of these biomarkers in hepatocellular carcinoma. Hepatol. Res. 46, 1380–1391. https://doi.org/10.1111/hepr.12687.

Subramani, T., Yeap, S.K., Ho, W.Y., Ho, C.L., Omar, A.R., Aziz, S.A., Rahman, N.M.A.N.A., Alitheen, N.B., 2014. Vitamin C suppresses cell death in MCF-7 human breast cancer cells induced by tamoxifen. J. Cell Mol. Med. 18, 305–313. https://doi.org/10.1111/jcmm.12188.

Sylvestre, M., Legault, J., Dufour, D., Pichette, A., 2005. Chemical composition and anticancer activity of leaf essential oil of *Myrica gale* L. Phytomedicine 12, 299–304. https://doi.org/10.1016/j.phymed.2003.12.004.

Sylvestre, M., Pichette, A., Longtin, A., Nagau, F., Legault, J., 2006. Essential oil analysis and anticancer activity of leaf essential oil of *Croton flavens* L. from Guadeloupe. J. Ethnopharmacol. 103, 99–102. https://doi.org/10.1016/j.jep.2005.07.011.

Tak, J., Sabarwal, A., Shyanti, R.K., Singh, R.P., 2019. Berberine enhances posttranslational protein stability of p21/cip 1 in breast cancer cells via down-regulation of Akt. Mol. Cell. Biochem. 1–11. https://doi.org/10.1007/s11010-019-03529-4.

Velauthapillai, N., Barfett, J., Jaffer, H., Mikulis, D., Murphy, K., 2017. Antioxidants taken orally prior to diagnostic radiation exposure can prevent DNA injury. J. Vasc. Interv. Radiol. 28, 406–411. https://doi.org/10.1016/j.jvir.2016.10.022.

Wang, H., Liu, X., Long, M., Huang, Y., Zhang, L., Zhang, R., Zheng, Y., Liao, X., Wang, Y., Liao, Q., 2016. NRF2 activation by antioxidant antidiabetic agents accelerates tumor metastasis. Sci. Transl. Med. 8 334ra351-334ra351. https://doi.org/10.1126/scitranslmed.aad6095.

Yap, T.A., Sandhu, S.K., Carden, C.P., de Bono, J.S., 2011. Poly (ADP-Ribose) polymerase (PARP) inhibitors: Exploiting a synthetic lethal strategy in the clinic. Ca - Cancer J. Clin. 61, 31–49. https://doi.org/10.3322/caac.20095.

Zha, J., Harada, H., Yang, E., Jockel, J., Korsmeyer, S.J., 1996. Serine phosphorylation of death agonist BAD in response to survival factor results in binding to 14-3-3 not BCL-XL. Cell 87, 619–628. https://doi.org/10.1016/S0092-8674(00)81382-3.

Zhang, Y., Zhang, Y., Yu, Y., 2017. Global phosphoproteomic analysis of insulin/Akt/mTORC1/S6K signaling in rat hepatocytes. J. Proteome Res. 16, 2825–2835. https://doi.org/10.1021/acs.jproteome.7b00140.

Zucman-Rossi, J., Villanueva, A., Nault, J.-C., Llovet, J.M., 2015. Genetic landscape and biomarkers of hepatocellular carcinoma. Gastroenterology 149, 1226–1239. e1224. https://doi.org/10.1053/j.gastro.2015.05.061.